International Journal of Surgery: Open Access

Global Scientific Library

Research Article

Identical Geometrical Profile for Both Craters and Arbitrary Long Incisions Produced by CO_2 Laser Beams onto Irradiated Biological and Non-biological Samples: The Importance of the Crater's Horizon Acceleration

Franco Canestri*

Research Fellow, University of Tel Aviv, Tel Aviv – Israel (1993-1994 and 2010) and National Cancer Institute, Milan - Italy (1982-1984)

Abstract

Background status: In order to forecast with sufficient precision the geometrical profile of a cut obtained via a moving surgical CO_2 laser beam emitting in Continuous Wave (CW), it is recommendable to produce a single crater with the same desired safety depth and acceptable superficial damage first.

This precaution allows to reduce the risks of starting an uncontrolled cutting process with unfavorable consequences: a single crater allows to test the selected laser set-up (output power, focal length and beam profile) under minimal damaging conditions in a volume with the same structural and thermodynamic characteristics of the cut and where no significant irreversible and permanent large damages can occur.

Goals and objectives: the next logical step is then to select a proper scanning speed of the same laser focal head and modified set-up over the surgical area to treat, which then would allow to produce a cut with the identical safe profile obtained with the single accepted test crater.

In more mathematical terms, the incognita to determine is the correct power density distributed over the complete desired cut length which produces the identical geometrical profile of the original test crater. As consequence, the correct "cut – speed" equation must guarantee the production of the original test crater profile all the way from the start to the end of the desired arbitrary incision.

Materials and methods: this Paper presents two separate analytical models and proposes some preliminary experimental results to be considered for both crater pre-testing and cut generation phases obtained via CW - CO_2 laser beams during forecasting and pre-simulations of challenging interventions in Operating Room.

Conclusion: the experimental evidence of the presence of an acceleration phase during the early crater production process in both biological and non-biological is presented and discussed as well.

Keywords: Crater; Incision; Cut; CO_2 Lasers; Continuous wave; PMMA; Power density; Speed; Focal head; Biological media; Geometrical profile; Horizon; Radius; Depth

Introduction

The CO_2 laser is one of the highest-powered and most efficient lasers that are currently available, and is one of the most useful in very many medical and surgical applications since more than 40 years [1-3].

Laser surgery uses an intensely and precisely focused beam at 10.6 μm to remove or vaporize tissue while controlling the bleeding in a wide variety of non-invasive and minimally invasive procedures. However, the invasive aspects of the laser beam below the surface to be treated generate all sorts of safety questions concerning the uncontrolled and invisible spreading of the beam near delicate vital organs while treating the volume of interest.

***Corresponding author:** Franco Canestri, Research Fellow, University of Tel Aviv, Tel Aviv, Israel and National Cancer Institute, Milan – Italy

Received: April 27 2017; **Accepted:** May 12 2017; **Published:** May 19 2017

The Author has already reported 16 several cases in which the clear presence of potential dangerous situations can raise safety alerts and recommend in-depth investigations.

A less invasive single crater on the mass to be treated simulates acceptable limiting geometrical boundaries and it can therefore be used as safety reference margin for more complex and challenging longer incisions near vital organs. These ones must be protected during any surgical procedures when CO_2 lasers are in use.

Material and Methods

A commercial TEM00- CO_2 laser has been coupled to regular focusing heads to be used for Continuous Wave (CW) laser beam delivery trials on *in-vitro* biological and non-biological samples. The TEM00 mode stands for "Gaussian Transversal Electromagnetic Mode" of the beam. Several experiments have been conducted (Tables 1 and 2) using particular combinations of laser optical parameters in output, depending on each case-by-case need. The total exposure time was kept to 10 sec. for the entire set of experiments. Several samples of the same tissue type have been irradiated under the same laser output conditions and all with the laser beam perpendicular to the surface and at the laser spot. All the irradiated samples have been considered for the final calculations and the resulting damage measurements.

Citation: Canestri F. Identical Geometrical Profile for Both Craters and Arbitrary Long Incisions Produced by CO_2 Laser Beams onto Irradiated Biological and Non-biological Samples: The Importance of the Crater's Horizon Acceleration. Int J Surg 2017; 1:101.

Five rabbits weighting 3 to 3.5 kilos have been sacrificed and 60 samples of trachea, myocardium, aorta and esophagus have been immediately excised, separated free of the adherent connective tissue and irradiated in the intima portion of the wall. The exposure distance above the surface to be irradiated was kept identical to the focal length of the lens in use. Each sample was examined in the fresh state and after the exposure to the laser irradiation for gross evidence of tissue charring black carbonized spots and craters. After irradiation all the *in-vitro* samples have been fixated immediately in buffered formalin for 72 hours, cleared with xylene, impregnated and embedded in paraffin and cut at 6 μm intervals. Each section was stained with hematoxyline / eozine and examined via optical microscopy. The slides were computer analyzed to measure the dimensions of the lesions, marked with '2R' for the diameter and 'Z' for the depth and photographed (Table 1 and Table 2). As control group, 10 plastic blocks (1 cm x 3 cm x 3 cm) have been irradiated with the same optical focusing heads in order to obtain clearer crater structures to allow better observation, more precise dimensional measurements and clearer comparison (Figure 1 and Figure 2).

These plastics chemically belong to the families of the Polymethil-Methacrylates (PMMA). Also, these experiments have been conducted to simulate the responses to the laser radiation of hard, low-water content tissues such as bone [3-5]. Also, these plastics are routinely used in orthopedic surgery as bone cement to repair severe fractures [5]. All the 'injury diameters 2R' and 'injury depths Z' reported in Table 1 and 2 are averaged over the number or experiments per type of tissue. Their tolerances are reported in % in Table 1 and 2 for all the samples and tests, including the PMMA ones. The PMMA samples show a compact and transparent hard structure [6] which allows very precise geometrical measurements.

In order to have a third control group for comparison, additional measurements with two focusing heads 2.5" and 5" focal lengths have been conducted. These measurements have been obtained by irradiating each sample perpendicularly and on the spot of each used focal.

The spot sizes are : 0.2 cm diameter of the spot produced by the 8.7" focal in TEM22 mode, 0.01242 cm diameter for the 2.5" focal and

Table 1: Irradiated Non-biological Media (PMMA) - all data in CGS Unit System. In yellow, samples with peculiarities. Preliminary data on minimal incision length (m = 2). For all samples : $V_{spot}\, t_{cut} = 2mR_{spot}$.

Media	*No. of Irradiated Samples (Craters)*	t_{cr} *given crater*	I_o *W / area spot on crater*	J_{cr} *given crater*	*Averaged* $Z_{cr}=Z_{cut}$ *over No. of Irradiated Samples(6% deviation)*	*Averaged* $2R_{cr}=2R_{cut}$ *over No. of Irradiated Samples (3% dev.)*	t_{cut} *to reach* Z_{cut}	V_{spot} *Speed of the Optical Head (Focal Spot) to generate the cut*	a_{acc} *of the Crater and Cut Depths Horizon* (Z_{cut}) *(start (*) / stop)*	J_{cut} *(m = 2)*
1. PMMA	12	1	17.21	2.5	0.02	0.09	1.88	0.43	5.46 / 0.011	16.5
2. PMMA	12	2	13.77	4	0.07	0.12	3.77	0.22	4.37 / 0.009	26.5
3. PMMA	12	4	8.6	5	0.11	0.19	7.53	0.11	2.73 / 0.0038	33.1
4. PMMA	5	0.1	6809	0.33	0.13	0.03	0.19	0.25	2167 / 7.36	2.17
5. PMMA	8	0.2	1708	0.66	0.03	0.1	0.38	0.25	542 / 0.39	4.37
6. PMMA	9	1	3105	6	0.21	0.1	1.84	0.05	985 / 0.12	39.7
7. PMMA	9	2	2587	10	0.3	0.13	3.77	0.02	821 / 0.04	66.2
8. PMMA	5	0.4	1708	1.32	0.05	0.09	0.75	0.12	542 / 0.164	8.73

Total samples: 72
all increasing except sample *b.*

(*) calculated via : $\left|\vec{a}_{media}\right| = \dfrac{W_{cr}}{\pi\tau_r A_e \rho R_{spot}^{\ 2}}$

Table 2: Irradiated Biological Media - all data in CGS Unit System. In yellow, samples with peculiarities. Preliminary data on minimal incision length (m = 2). For all samples : $V_{spot}\, t_{cut} = 2mR_{spot}$.

Media	*No. of Irradiated Samples (Craters)*	t_{cr} *given crater*	*Io W / area spot on crater*	J_{cr} *given crater*	*Averaged* $Z_{cr}=Z_{cut}$ *over No. of Irradiated Samples (9% deviation)*	*Averaged* $2R_{cr}=2R_{cut}$ *over No. of Irradiated Samples (6% deviation)*	t_{cut} *to reach* Z_{cut}	V_{spot} *Speed of the Optical Head (Focal Spot) to generate the cut*	a_{acc} *of the Crater and Cut Depths Horizon* (Z_{cut}) *(start (*) / stop) x 10 exp(-3)*	J_{cut} *(m = 2)*
a. Trachea	8	0.4	34.4	2	0.02	0.03	0.75	1.08	2.1 / 56	13.2
b. Myocard.	5	4	34.4	20	0.01	0.11	7.54	0.11	2.1 / 0.29	132
c. Esophag.	6	0.2	34.4	1	0.05	0.12	0.38	2.15	2.1 / 661	6.62
d. Esophag.	9	0.2	44.8	1.3	0.06	0.14	0.38	2.15	2.8 / 859	8.6
e. Esophag.	9	1.5	44.8	9.75	0.08	0.15	2.83	0.28	2.8 / 18.78	64.6
f. Aorta	10	0.5	22.7	1.65	0.08	0.08	0.94	0.86	1.4 / 169	10.9
g. Aorta	10	1.5	22.7	4.95	0.03	0.11	2.83	0.28	1.4 / 7.51	32.8

all increasing
except sample *b.*

(*) calculated via : $\left|\vec{a}_{media}\right| = \dfrac{W_{cr}}{\pi\tau_r A_e \rho R_{spot}^{\ 2}}$

Citation: Canestri F. Identical Geometrical Profile for Both Craters and Arbitrary Long Incisions Produced by CO_2 Laser Beams onto Irradiated Biological and Non-biological Samples: The Importance of the Crater's Horizon Acceleration. Int J Surg 2017; 1:101.

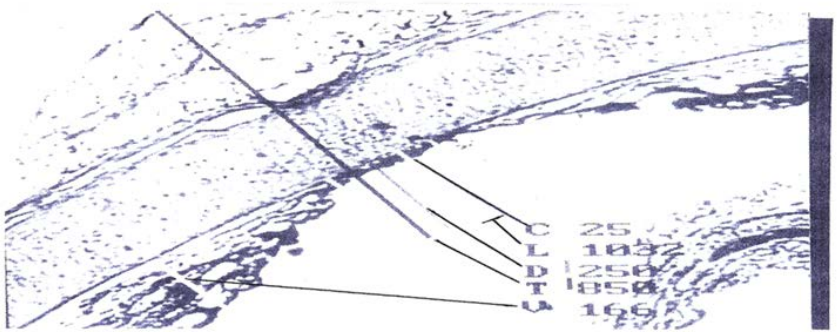

Figure 1: Rabbit trachea ring irradiated by a co_2 laser beam.

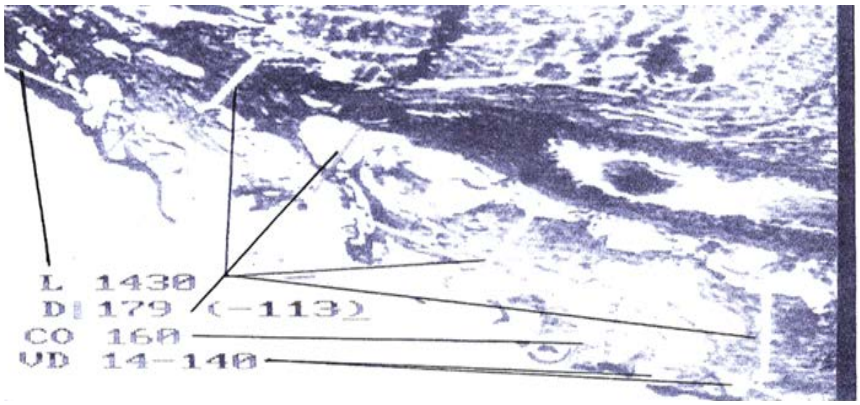

Figure 2: Rabbit myocardium.
Legenda: V = vacuolization layer, C = carbonization
L = crater/ lesion diameter, D = cr./les. Depth.
T = total sample thickness, C_o = necrosis of coagulation
VD = diameter of the vacuoles
All the dimensions are in microns.

0.02484 cm for the 5“ focal, both for TEM00 Gaussian mode. Only the three types of plastics have been used at 2.5” and 5” focal: due to the high power density on the beam spot caused by these two specific focal lengths, this decision was necessary not to cause too destructive thermodynamic damages on the biological sample.

Discussion about the two models: A) the speed- versus B) the global-based approaches.

A) The fundamental starting consideration is to make sure that the same laser beam power density $I_{\max}\left(Watt/spot\ area = Joules/time \times spot\ area\right)$ for both single crater and cut generation procedures gets delivered on the surface to be treated in order to create the same safety sublimated profile in both circumstances. Two additional assumptions are: the spot area is circular and the scanning speed $\left|\vec{V}\right|$ of the focusing head is constant.

Based on this, the key mathematical equations to consider are:

$$I_{crater} = \frac{J_{cr}}{t_{cr}\pi R_{spot}^2} \tag{1}$$

$$2R_{spot} = \left|\vec{v}\right| t_{cut} \tag{2}$$

The basic condition to respect in order to achieve the same geometrical “diameter – depth” profile for both single crater and arbitrary cut is to deliver the same power density $\boldsymbol{I}_0$ (W / cm^2) on the same laser spot size.

The laser can have different focal lengths $\boldsymbol{f}_x$, different wavelength λ and different beam profiles (TEM = Transverse Electromagnetic Mode), therefore the power density for both crater and cut generation procedures can be written from Eq. (1) and (2) as follows:

$$\frac{J_{cr}}{t_{cr}\pi {R_{spot}}^2} = \frac{4J_{cut}}{t_{cut}\pi \left|\vec{v}\right|^2 {t_{cut}}^2} \tag{3) a, b}$$

$$2R_{spot} = \frac{4f_x M^2 \lambda_{o_2}}{\pi D_0} = \frac{4f_x (2n_j + 1)\lambda_{o_2}}{\pi D_0}$$

Where the diameter of the spot size for a CO_2 laser beam is:

where $\boldsymbol{J}$ is the selectable output energy in Joules, $\boldsymbol{R}_{spot}$ is the spot of the focal in-use and $\left|\vec{V}\right|$ is the scanning speed of the focusing head transiting over the surgical area.

$\boldsymbol{D}_0$ is the diameter of the laser beam before passing through the focusing lens of the laser focusing head (data provided by the Laser Manufacturer) while the numerical factor ‘n’ is the number of modes of beam in use: for a large TEM laser beams, n= 5 has been used while for the TEM00 Gaussian mode we must use n = 0 at all times [7,8].

Moreover $\boldsymbol{t}_{cr}$ is the total exposure time on a single $\boldsymbol{2R}_{spot}$-diameter spot, $\boldsymbol{t}_{cut}$ is the time required to pass over any arbitrary $\boldsymbol{2R}_{spot}$-diameter-long section contained in the total cut length to be produced, $\boldsymbol{J}_{cr}$ is the total energy in Joules delivered over the spot and $\boldsymbol{J}_{cut}$ is the total energy delivered by the moving focusing head while scanning any arbitrary

$2R_{spot}$-diameter-long section of the total cut (Figure 1) in order to obtain the same geometrical profile of the single crater.

From Eq. (3a), the required J_{cut} as function of the scanning speed is:

$$J_{cut} = \frac{J_{cr} t_{cut}^{\ 3} |\vec{v}|^2}{4 t_{cr} R_{spot}^{\ 2}} \quad (4)$$

As shown in Figure 3, the heath conduction modalities on the crater and on the cut are completely different, meaning that small parts of energy are gradually but rapidly taken away from the surface of interest while the focusing head is transiting over the surface.

These small quantities do not contribute to the generation of the crater: therefore, in order to achieve the same geometrical profile, the energy delivered on the cut must be higher than the one need for the single reference crater. Here, the heath conduction is stable and therefore the remaining energy in Joules is piling-up to the quantity needed to create the reference crater profile to be used later for the cut production.

This means from Eq. (4):

$$\frac{t_{cut}^{\ 3} |\vec{v}|^2}{4 t_{cr} R_{spot}^{\ 2}} > 1 \quad (5)$$

Another important consideration must be considered now. The vertical acceleration [10] of the crater development along the Z coordinate (crater depth – Table 1 and Table 2) can be used to define the upper limit of the required exposure time for the cut development process.

Therefore from Eq. (4) and Eq. (5), all these considerations lead to:

$$t_{cut\,\min} = \sqrt[3]{\frac{4 t_{cr} R_{spot}^{\ 2}}{|\vec{v}|^2}} = \frac{2R_{spot}}{|\vec{v}|} \quad (6)$$

While the boundary conditions given by the experimental results on the selected media can be considered this way (uniformly accelerated motion model):

$$t_{cut} = \sqrt{\frac{2Z_{cr}}{|\vec{a}_{medium\ Z_{cr}}|}} > t_{cut_{\min}} = \sqrt[3]{\frac{4 t_{cr} R_{spot}^2}{|\vec{v}|^2}} \quad (7)$$

This is needed in order to allow $J_{cut} > J_{crater}$, as described in Eq. (5) and in Figure 4.

Here, the peak vertical acceleration (10) of the crater for the irradiated media is:

$$|\vec{a}_{media}|_{\max} = \varepsilon \frac{4k\alpha^2}{\pi A_e \rho R_{spot}^{\ 2}} \frac{J_{cr}}{t_{cr}} = \varepsilon \frac{W_{cr}}{\pi \tau_r A_e \rho R_{spot}^{\ 2}} \quad (8)$$

Assuming that the acceleration of the crater depth production is constant (Table 1 and Table 2).

ε, α, ρ, τr, k and ***Ae*** are all thermodynamic parameters described with greater details by the Author is several Publications already [10,11], including the fact that ***ε*** = 1 along the Z coordinate and in the range of 0.5-0.8 for the X,Y ones [11]. By using the experimental results presented in this Paper, the correct value is 0,55 +/- 10% for non-biological media (PMMA) but no precise limit can be given for the biological ones, where the inherent bio-chemical characteristics of each sample are very dependent on the structure of the irradiated one. This fact is related to the large uncertainty amongst the resulting acceleration values measured on different samples.

The theoretical value presented by the Author in [10,11] is equal to 0,88 for the PMMA.

We can define the following numerical parameter as follows (Figure 6a):

$$m \equiv \frac{L_{cut}}{2R_{0spot}} \geq 2 \quad (9)$$

Now, both cut and crater have the same profile if the power density is the same:

$$\frac{W_{0cr}}{\pi R_{0spot}^{\ 2}} = \frac{W_{cut}}{2R_{0spot} L_{cut} + \pi R_{0spot}^{\ 2}} \quad (10)$$

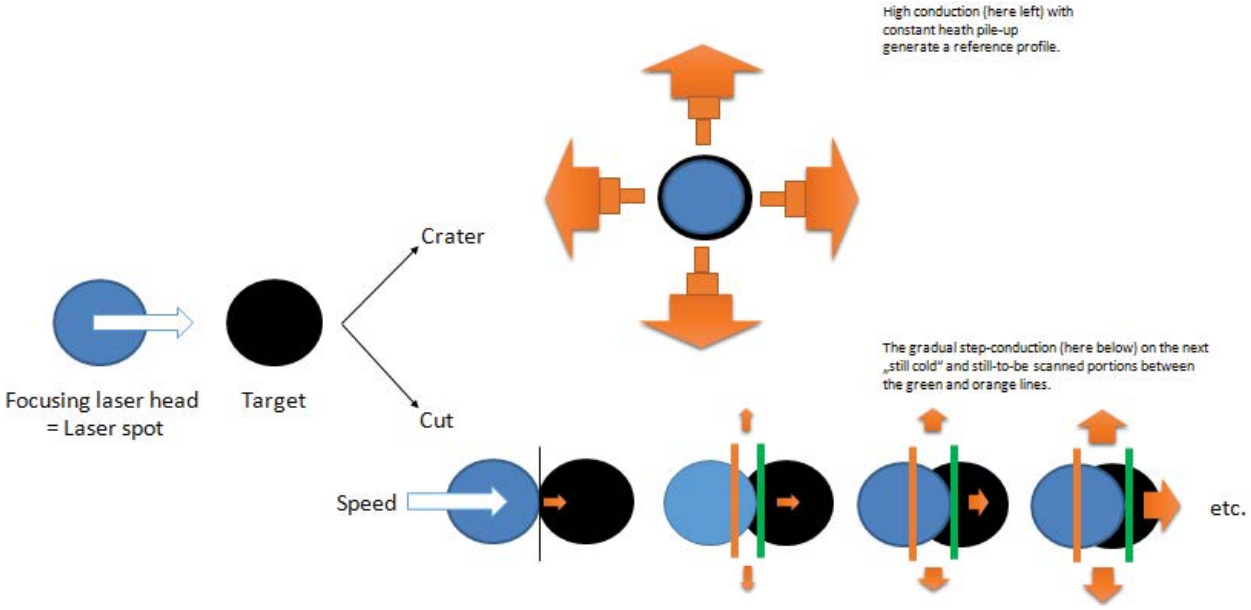

Figure 3: Heath conduction modalities (red arrows) between scanning (cut) and fixed (crater) focusing head on the spot. The heath quantities conducted away from the target do not contribute to the sublimated crater profile. During the formation of the crater, the conducted heath increases over the same geometry, not like in the cut mode.

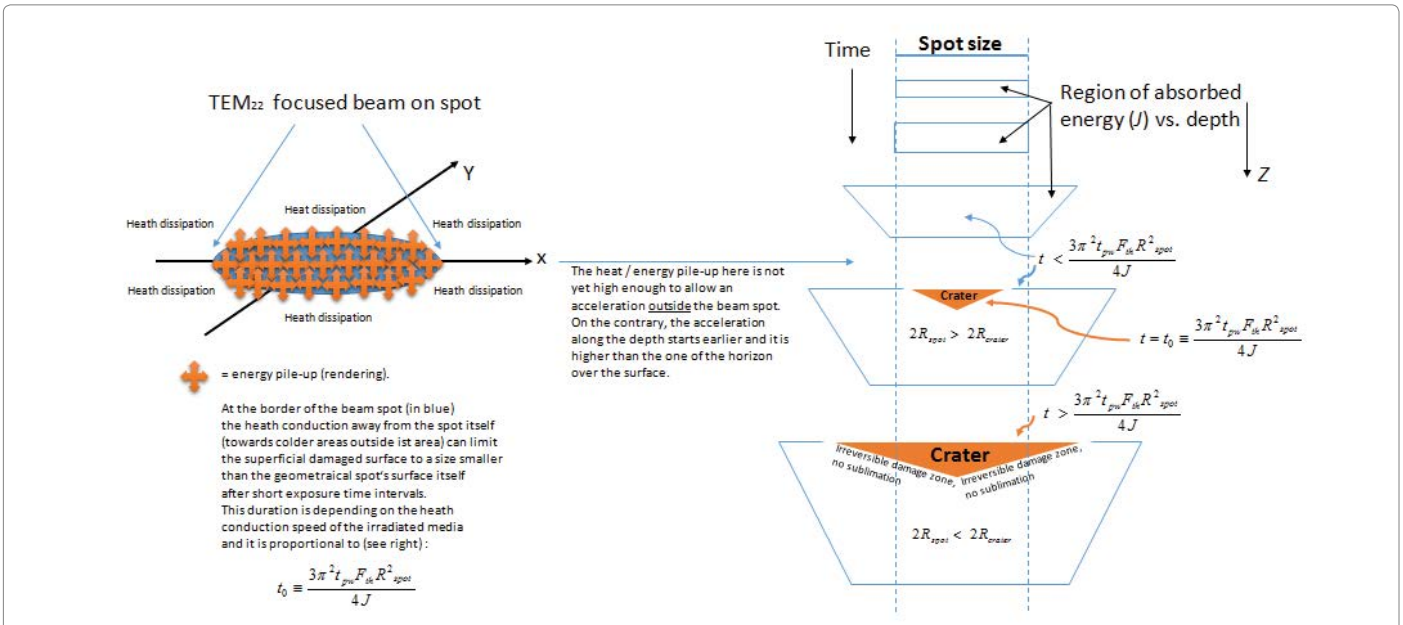

Figure 4: Heath conduction modalities (red arrows) and the beginning the ablation process.

where "0" indicates the known magnitudes (a-priori selected or calculated by the user).

By using Eq. (9) we can easily calculate:

$$W_{cut} = 2\frac{W_{0cr}}{\pi R_{0spot}}(2mR_{0spot}) + W_{0cr} = \frac{4mW_{0cr}}{\pi} + W_{0cr} \quad (11a)$$

which allows us to find via Eq. (4) the relationship valid for any $2R_{spot}$ -crater along the cut :

$$\frac{W_{cut}}{m} = \frac{4W_{0cr}}{\pi} + \frac{W_{0cr}}{m} = \frac{W_{0cr} t_{cut}^2 |\vec{v}_0|^2}{4mR_{0spot}^2} \quad (11b)$$

The two unknowns t_{cut} and the acceleration 'a' can be obtained via the following system:

$$\frac{4}{\pi} + \frac{1}{m} = \frac{t_{cut}^2 |\vec{v}_0|^2}{4mR_{0spot}^2}$$

$$t_{cut} = \sqrt{\frac{2Z_{0cr}}{\left|\vec{a}_{medium_{Z_{0cut}}}\right|}} \quad (12) \text{ a, b}$$

The suffix "cut" for the acceleration is now needed in order to underline the parallelism (Figure 5 and Figure 6) "crater – cut" for the same desired crater-cut profile onto the selected media:

$$\left|\vec{a}_{medium_{Z_{0cut}}}\right| = \frac{2Z_{0cr}|\vec{v}_0|^2}{m(2R_{0spot})^2}\frac{1}{\frac{4}{\pi}+\frac{1}{m}} = \frac{2Z_{0cr}}{t_{2R_{spot}}^2}\frac{1}{m(\frac{4}{\pi}+\frac{1}{m})} \to 0 \quad if \quad m \to \infty \quad (13)$$

For $m \to 1$, the following single crater's horizon acceleration (at Z_0) can be expected:

$$\lim_{m\to 1}\left(\frac{2Z_{0cr}}{t_{2R_{spot}}^2}\frac{1}{m(\frac{4}{\pi}+\frac{1}{m})}\right) \cong \frac{Z_{0cr}}{1{,}135 \cdot t_{2R_{spot}}^2} \approx \left|\vec{a}\right|_{Z_0} \equiv \left|\vec{a}\right|_{stop}$$

This approximation must be validated with more precision for PMMA *vs.* biological media.

B) In order to further analyze the cut development along its length L in a more global manner and then compare the results from both approaches, we can say that both power densities after the crater and after the cut (m = 2) production must be equal:

$$\frac{W_{cr_0}}{\pi R_{spot}^2} = \frac{\left(\frac{J_{cut\_x}}{t_{cr_0} + t_{cut\_sel}}\right)}{4R_{spot}^2 + \pi R_{spot}^2} \quad (14)$$

The case here reported simulates the basic reference cut obtained with m=1.

The unknown is J_{cut_x} and it has to be equal to the one calculated via Eq. (4). Without any corrective measures, each single systematic error on J_{cut} (for the entire set of experiments (Table 1 and Table 2)) between Eq. (4) and Eq. (14) is less than 0,5% : a very small and constant value that points out to the same representation of the all experimental conditions (Table 1 and Table 2).

If the sweeping time over the spot arbitrary changes, then the power density on the spot changes as well, causing complex cross-modifications in all the equations reported above and ultimately resulting in the wrong generated cut profile (Figure 6). In-fact, the outcomes of Equations (1) to (13) have to be considered related only to one selected laser set-up:

Therefore, a new laser set-up generates its own new and different set of data.

Consequently and logically, only one acceleration value of the crater horizon must then correspond to each selected laser set-up itself.

Instead, from Eq. (13) there are two of them:

i) One obtained for m = 2, which means "shortest possible cut = 2 x crater", following

Eq. (2) in order to have an absolute initial speed reference, and

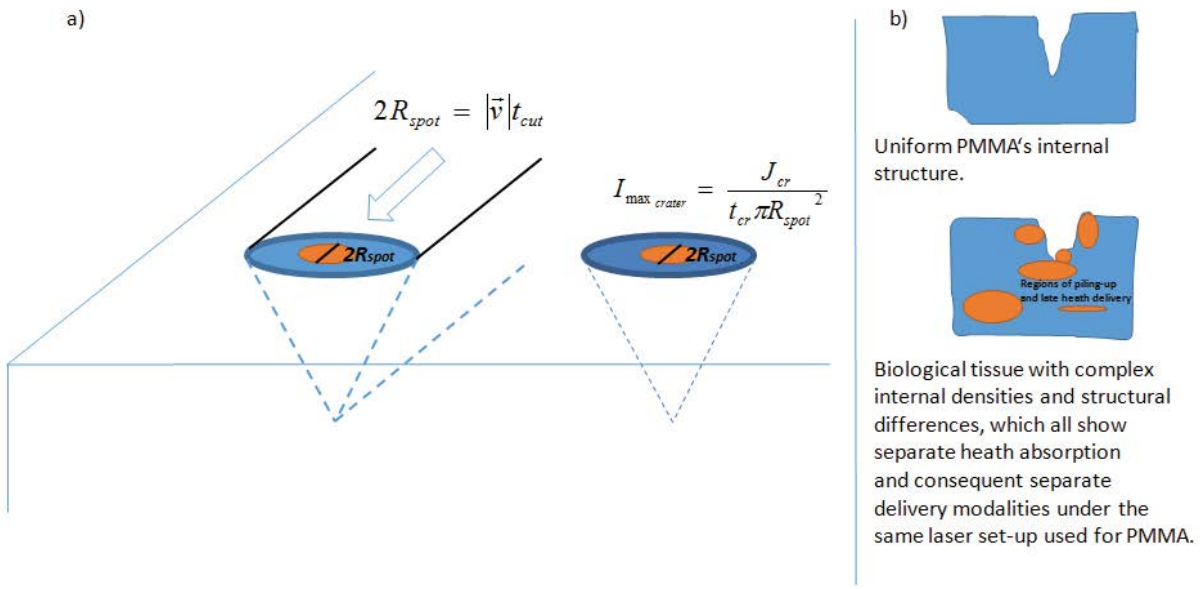

Figure 5: Three dimentional rendering of craters versus cuts, depending (b)) on biological or non-biological tissue characteristics. For very long incisions, the lens geometry can vary, meaning that the spot size increases due to long exposure to heath.

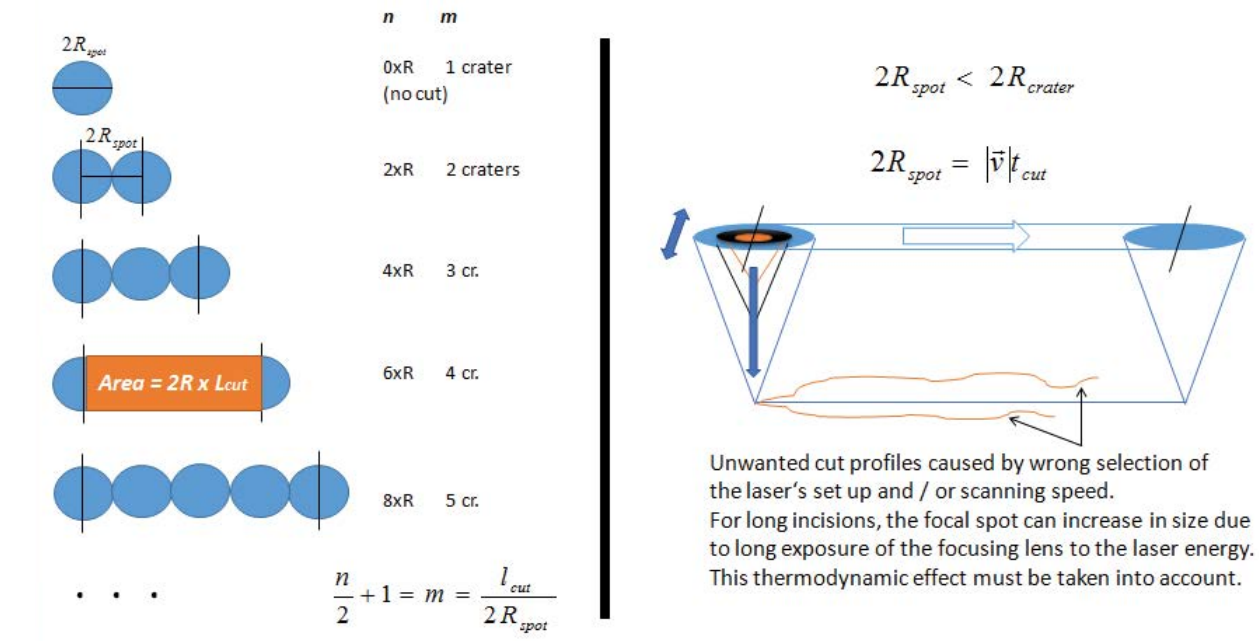

Figure 6 a,b: Schematic rendering for a constant speed simulation of the scanning focal head.

ii) The other one obtained for $m \to 00$, which means "longest possible cut".

The numerical difference between the two is large, in contrast to the fact that there must be only one referenced to the shortest possible cut (1 x crater, case a)). The reason is that Equation (13) does not take into consideration that "very long cut" correspond to "very long beam exposure" of the laser lens to the beam, meaning that larger and larger heath quantities are absorbed by the lens itself. This results into non-linear geometrical modifications of the it (see both f_x and $(2n_{ij} + 1)$ in Eq. (3) b), causing therefore an enlargement of its focal spot for the same beam aperture D_0. The same output energy on a larger and larger focal spot (lower and lower power density) reduces the penetration capability of the beam itself, causing therefore a lower and lower vertical acceleration of the crater's horizon.

Following these considerations, the presence of acceleration has been experimentally demonstrated in the present Study and the different behavior of the accelerated crater growth across several different irradiated media has been confirmed as well.

For all the cases reported in Table 1 and 2, the following relationship for m = 2 are satisfied:

$$m \cdot 2R_{spot} = 4R_{spot} = |\vec{v}|t_{cut} \quad (15)$$

More investigations are needed to confirm all these conclusions with stronger evidence on a larger set of biological media and for longer cuts with m >> 2, therefore with $L_{cut} >> 2R_{spot}$.

In case of any arbitrary speed of the focusing head, then the comparison to a single safe crater as initial starting reference point cannot be used any longer (this study).

Citation: Canestri F. Identical Geometrical Profile for Both Craters and Arbitrary Long Incisions Produced by CO_2 Laser Beams onto Irradiated Biological and Non-biological Samples: The Importance of the Crater's Horizon Acceleration. Int J Surg 2017; 1:101.

This different "cut-first-to-crater" approach (based on Eq. 10 as starting point) requires additional separate investigations which will be presented and discussed by the Author in the near future.

Global Discussion about both Models A) and B)

This Paper presents a comprehensive workflow which can be summarized in the following way: when the laser beam's focal spot starts to scan the surface to be treated at a constant speed "v", then the output energy must be enhanced from "J_{cr}" to "J_{cut}" within the time slot of max. "t_{cut}" seconds. This will produce a cut with the same geometrical profile of the crater previously obtained during "t_{cr}" and with "J_{cr}" into the same media and with the same optical set-up. It is interesting to observe (Table 2) that the starting acceleration along the Z coordinates in PMMA samples is larger than the one at the bottom of the crater or cut: In biological tissue the opposite happens, although over a very limited geometrical range.

The constant polymeric structure of the PMMA allows an uniform accumulation of heath and consequent smooth ablation also due to its low water content. On the contrary, the higher fluids content of complex biological tissues requires longer initial time for the transition to boiling and evaporation first, then to carbonization and finally to ablation, leading to an increase of acceleration of the energy piled-up energy and its consequent avalanche effect once the ablative phase has become steady during "beam on". Fat, liquids, hard tissues and muscles accumulate energy differently and without any thermodynamic changes until a critical limit is reached, causing a sudden punctual "explosion-like" heath delivery along both vertical, diagonal and horizontal directions (Figure 5b)) [12-15].

In other words, the polymers start to ablate very quickly and to dissipate heath uniformly during irradiation also. The biological tissues instead cumulate energy for a certain period of time until the first ablation takes place, then a sort of explosion follows, as demonstrated by the Author in [16] as well. The process then continues by releasing all the piled-up energy. This phase corresponds to the increase of the acceleration of the crater horizon, as here clearly demonstrated: for the same laser set-up, the overall depth is smaller but growing at higher acceleration than in the PMMA, which shows rather the opposite behavior.

Now looking at the other results reported in Table 1 and Table 2, similar power densities on the spot generate very different J_{cut} requirements and associated acceleration values, depending on the type of the biological media, but mainly on the quantity of irradiated muscular and fat tissue [17]. On PMMA samples, very high power densities generate lower and more uniform demand of J_{cut}, mainly due to its internal homogeneous structure. For all the irradiated media under very different laser set-ups, t_{cut} oscillates in a very stable manner between 0.1 and 7.5 seconds even considering the non-biological PMMA samples. Particular cases have been marked in yellow on both Tables.

Conclusion

This procedure allows also to numerically quantify the crater horizon's acceleration: once more it demonstrates the existence of this important parameter which was theoretically postulated by the same Author in other previous studies [9-11]. Still, it is important to mention again that the PMMA has a constant geometrical and thermochemical structure and it can therefore generate equal outcomes in Joules based on pure geometrical assumptions only.

More investigations are needed in order to further improve the quality of this preliminary methodology and improve the consistency of the results over very long incisions.

Acknowledgment

This Paper is dedicated to Mrs. Sabine and Mathelda Canestri.

References

1. Laufer G. 1983. Primary and Secondary Damage to Biological Tissue induced by Laser Radiation. Applied Optics. 22: 676-681.
2. Clayman L, Fuller T, Beckman H. 1978. Healing of Continuous-Wave and Rapid Superpulsed, Carbon Dioxide, Laser- induced Bone Defects. - J Oral Surgery. 36: 932-937.
3. Canestri F. 1992. Proposal of a computerized algorithm for CW CO_2 laser on-line control during orthopaedic surgery. Phase I: theoretical introduction and first *in-vitro* trials. - Int J Clin Mon Comp. 9: 1-44.
4. Canestri F. 1997. Proposal of a computerized algorithm for continuous wave CO_2 laser on-line control during orthopedic surgery. Phase II: Simplified algorithm version (LCA-s) and helmet-mounted data access device solution. Int J Clin. Mon and Comp. 14: 199-206.
5. Scholz C. et al. 1991. Die Knochenzemententfernung mit dem Laser. Abstract in English – Biomed. Technik (in German Language). 36: 120-128.
6. Canestri F. 1988. A proposed Clinical Application of a Model of CO_2 Laser Radiation Induced Damage Craters. J Med Eng. Techn. 12: 112-117.
7. TF Johnston. 1998. Beam propagation (M2) measurement made as easy as it gets: the four-cuts method. Appl. Opt. 37: 4840.
8. ISO Standard 11146. 2005. Lasers and laser-related equipment – Test methods for laser beam widths, divergence angles and beam propagation ratios.
9. Canestri F. 2011. Accurate quantification of the Optical Absorption Coefficient and of the Thermal Relaxation Time for PMMA and for low-water-content media during early ablation with CO_2 laser-beam at the wavelength of 10.6 microns. Photom. Laser Surg. 29: 61-66.
10. Canestri F. 2014. Acceleration Bursts of the Crater's Horizon at Each On-set of Pulsed CO_2 Laser Ablation into PMMA Samples. Lasers in Medicine. 6.
11. Canestri F. 2011. Ultra-Conservative Minimally Invasive Surgery (UCMIS) with Pulsed Non-Gaussian CO_2 Laser Beams Focused Through the Shortest Possible Focal Length. Photomedicine and Laser Surgery. 29: 759-766.
12. Li li, et al. 2014. Analysis of thermal conductivity in living biological tissue with vascular network and convection. Int J Thermal Sciences. 86: 219-226.
13. Whiting, P. et al. 1992. "A One-Dimensional Mathematical Model of Laser Induced Thermal Ablation of Biological Tissue." - 'Lasers in Medical Sciences." 7: 357-368.
14. Kyunghan Kim, Zhixiong Guo. 2006. Thermal Relaxation Times in Biological Tissue Subjected to Pulsed Laser Radiation. 9th AIAA / ASME Joint Thermophysics and Heath Transfer Conference, San Francisco. 2938.
15. Walsh JT, Flotte TJ, Deutsch TF. 1989. "Er: YAG Laser Ablation of Tissue: Effect of Pulse Duration and Tissue Type on Thermal Damage. Laser in Surg. and Med. 9: 314-326.
16. Canestri F. 2002. Sudden and unpredictable below-surface ablation pattern changes by CO_2 laser beams: a qualitative description of five macroscopic cases observed in PMMA with high probability to occur during surgery in low-water-content tissues. J Clin Las Med and Surg. 20: 335-339.

17. Zhao-Zhang Li, Reinisch L, Van de Merwe WP. 1992. "Bone Ablation with Er: YAG and CO_2 Laser: Study of Thermal and Acoustic Effects. Las. In Surgery and Med. 12: 79-85.

18. Canestri F, Katzir A, et al. 1994. Pulsed CO_2 laser beam delivery and real time temperature Measurements. SPIE Laser-Tissue Interaction Congress, Los Angeles. 2134A: 477.